Supplemental Figures

Figure S1

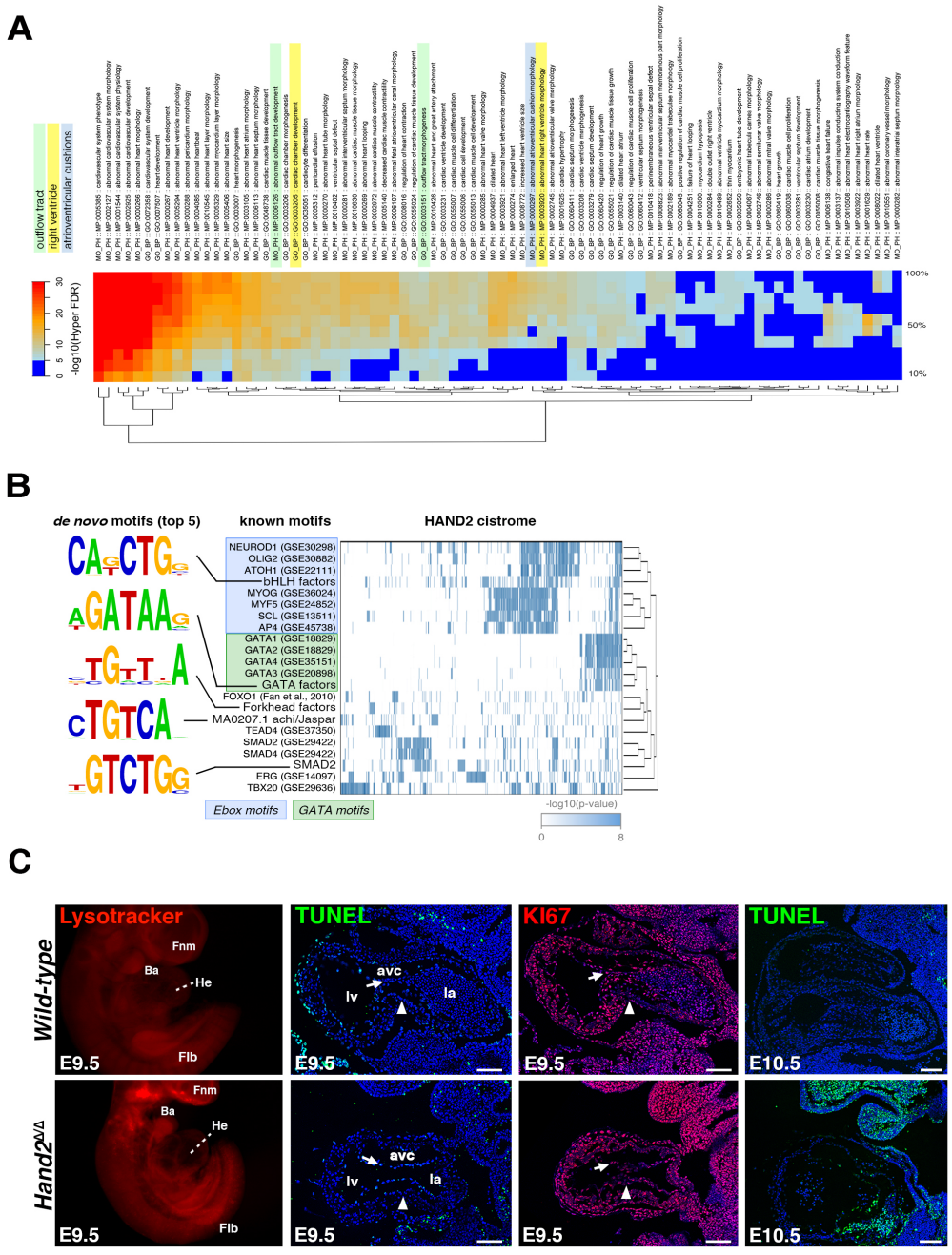

Figure S1 (related to Figure 1). Analysis of the genomic regions enriched in HAND2 chromatin complexes and associated genes.

(A) Heat map showing the enrichment of heart-related GO term categories in the list of putative HAND2 target genes defined by GREAT analysis. The columns denote ten incremental bins of HAND2-bound regions (from 10% to the complete set = 100%). For visualization, hyper-geometric p-values equal or lower to 1e-30 were set to this value. Terms were hierarchically clustered and re-ordered according to the row-wise mean. GO terms related to the development of specific cardiac compartments are highlighted by different colors: outflow tract (green), right ventricle (yellow) and atrioventricular cushions (blue). While the general cardiac terms are systematically identified in each

incremental bin (top term: cardiovascular system phenotype), GO terms related to more specific aspects of cardiac development (such as: abnormal heart right ventricle morphology) are only detected when considering an increasing number of peaks or the entire dataset. (B) Hierarchical clustering of the high-affinity matches for each of the enriched known motifs across the HAND2-contacted regions is shown. The top five binding motifs that were identified *de novo* are highlighted on the left. (C) Analysis of the patterns of cell death in *Hand2*-deficient mouse embryos. Panel Lysotracker: whole mount Lysotracker staining reveals increased apoptosis in branchial arches (Ba) and frontonasal mass (Fnm) of mutant mouse embryos at E9.5 (red fluorescence), while no aberrant apoptosis is detected in the developing heart. He: heart; Flb: forelimb bud. Panel TUNEL: analysis of serial section by TUNEL staining confirmed that apoptosis in not increased in the mutant heart at E9.5 (TUNEL positive cells fluoresce green). Panel KI67: the majority of all cells are KI67 positive (red fluorescence), which indicates that there is no major effect on cell proliferation in mutant hearts at E9.5. Right-most panel TUNEL: Only by E10.5, the apoptosis is significantly increased in mutant hearts in comparison to wild-type controls. Representative images are shown for all samples analyzed (n=3). avc: atrioventricular canal; lv: left ventricle; la: left atria; oft: outflow tract.

Figure S2

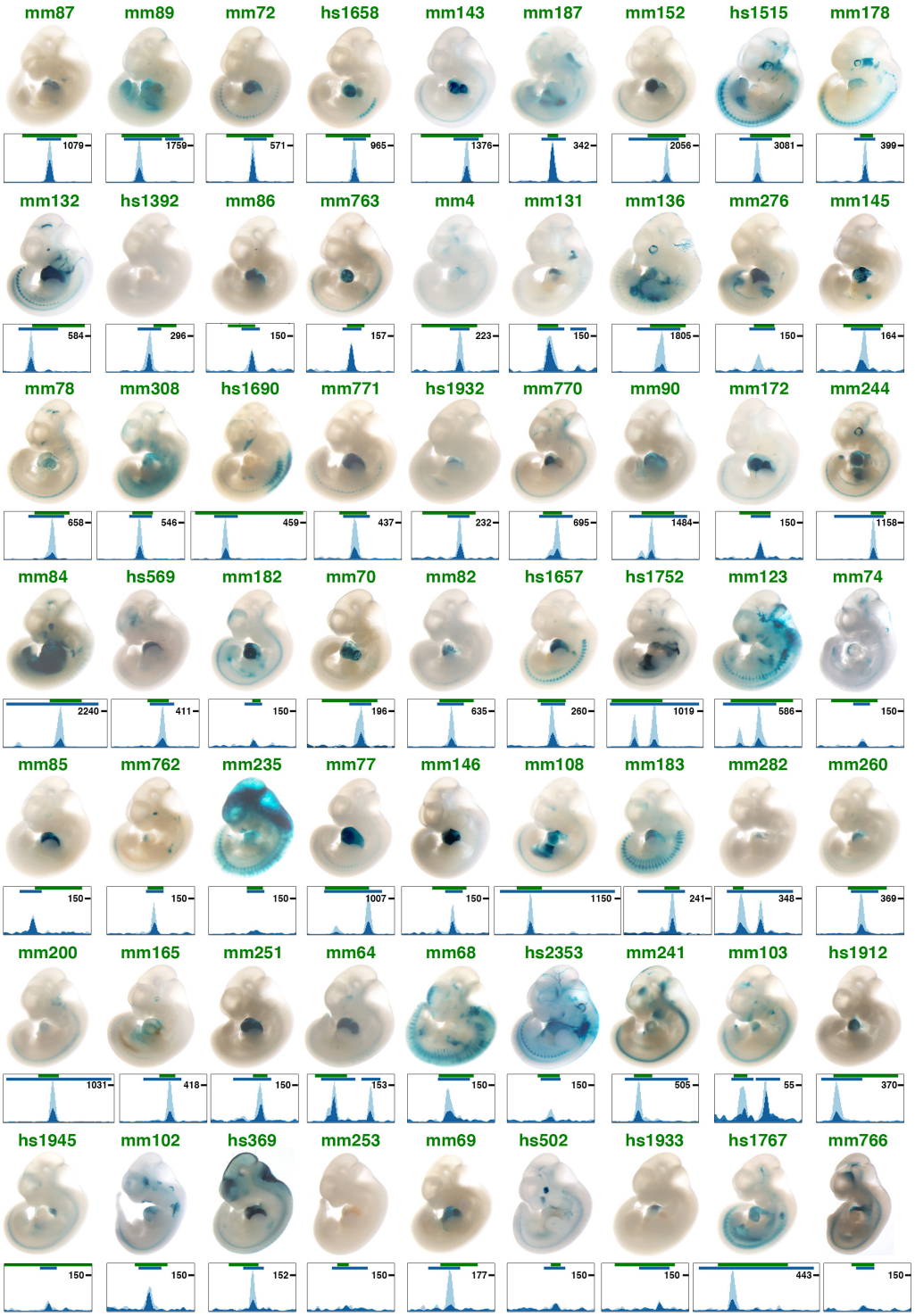

Figure S2 (related to Figure 1). Activities of the VISTA cardiac enhancers that overlap genomic regions enriched by HAND2 ChIP-Seq (E10.5).

Representative transgenic founder embryos from the public VISTA enhancer database collection (https://enhancer.lbl.gov; Visel et al., 2007) are shown. The transgenic embryos were not generated as part of this study, but images from the database collection were used for the purpose of this analysis. For each VISTA enhancer, the HAND2 ChIP-Seq peak identified by MACS analysis is indicated by a blue bar. The genomic regions used for *LacZ* reporter analysis are indicated by a green bar. mm: mouse element; hs: human element. Nomenclature used is according to the VISTA database.

Figure S3

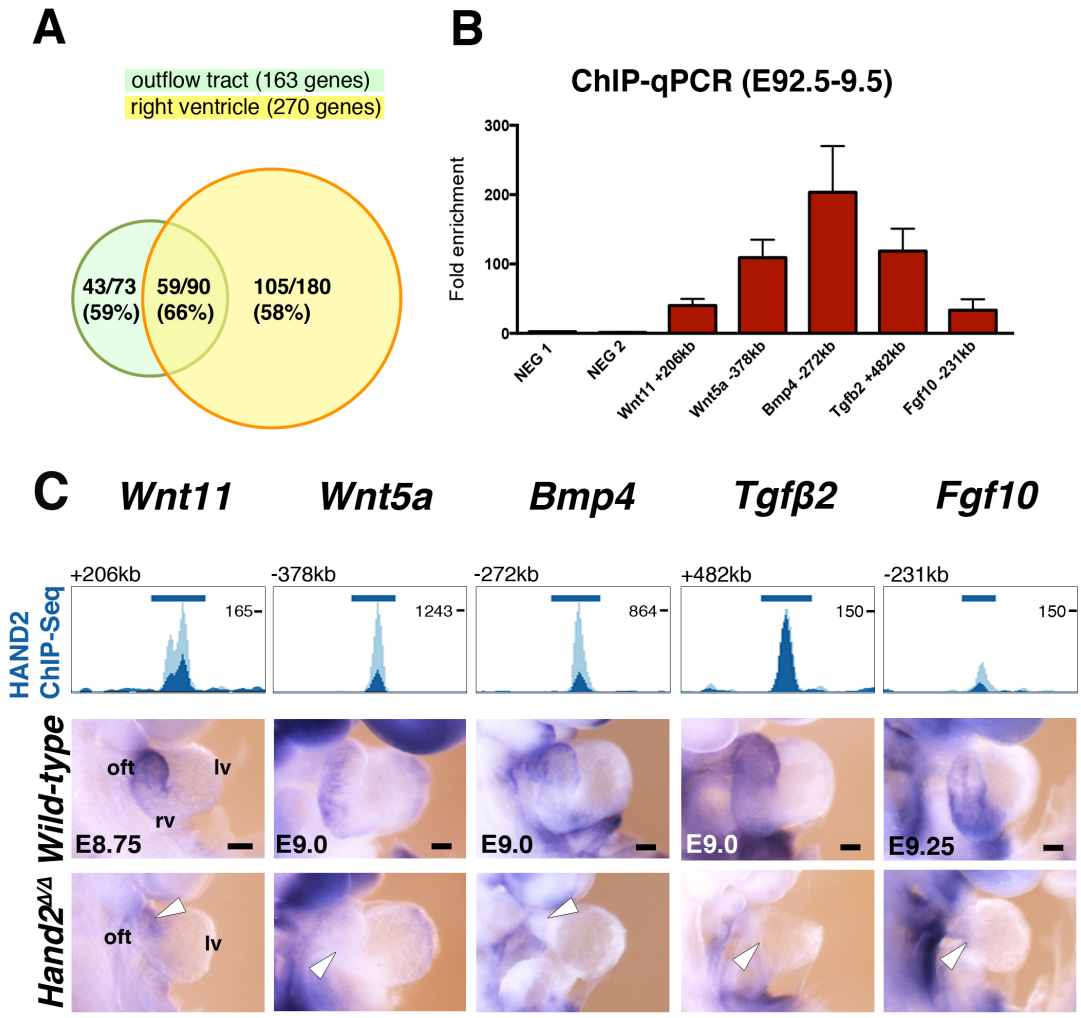

Figure S3 (related to Figure 1). HAND2 target genes encoding ligands for signaling pathways that function in OFT and/or right ventricle morphogenesis.

(A) Venn diagram shows the intersection of genes associated with the following mouse phenotype and GO terms, respectively: MP:0006126: abnormal outflow tract development; MP:0003920: abnormal heart right ventricle morphology; GO:0003151: outflow tract morphogenesis; GO:0003205: cardiac chamber development. Numbers and percentages indicate how many of the genomic landscapes associated to the terms encode regions enriched in HAND2 chromatin complexes. (B) ChIP-qPCR validation of HAND2 target regions associated to genes encoding ligands in embryonic hearts at E9.25 (n=2; mean ± SD). (C) Comparative WISH analysis of HAND2 target genes encoding signaling ligands in wild-type and *Hand2*-deficient mouse embryos. Graphs show the highest enriched HAND2 ChIP-Seq peaks associated with the genes analyzed. White arrowheads: reduction/loss of expression in *Hand2*-deficient embryos. oft: outflow tract, rv: right ventricle, lv: left ventricle. Scale bar: 100µm.

Figure S4

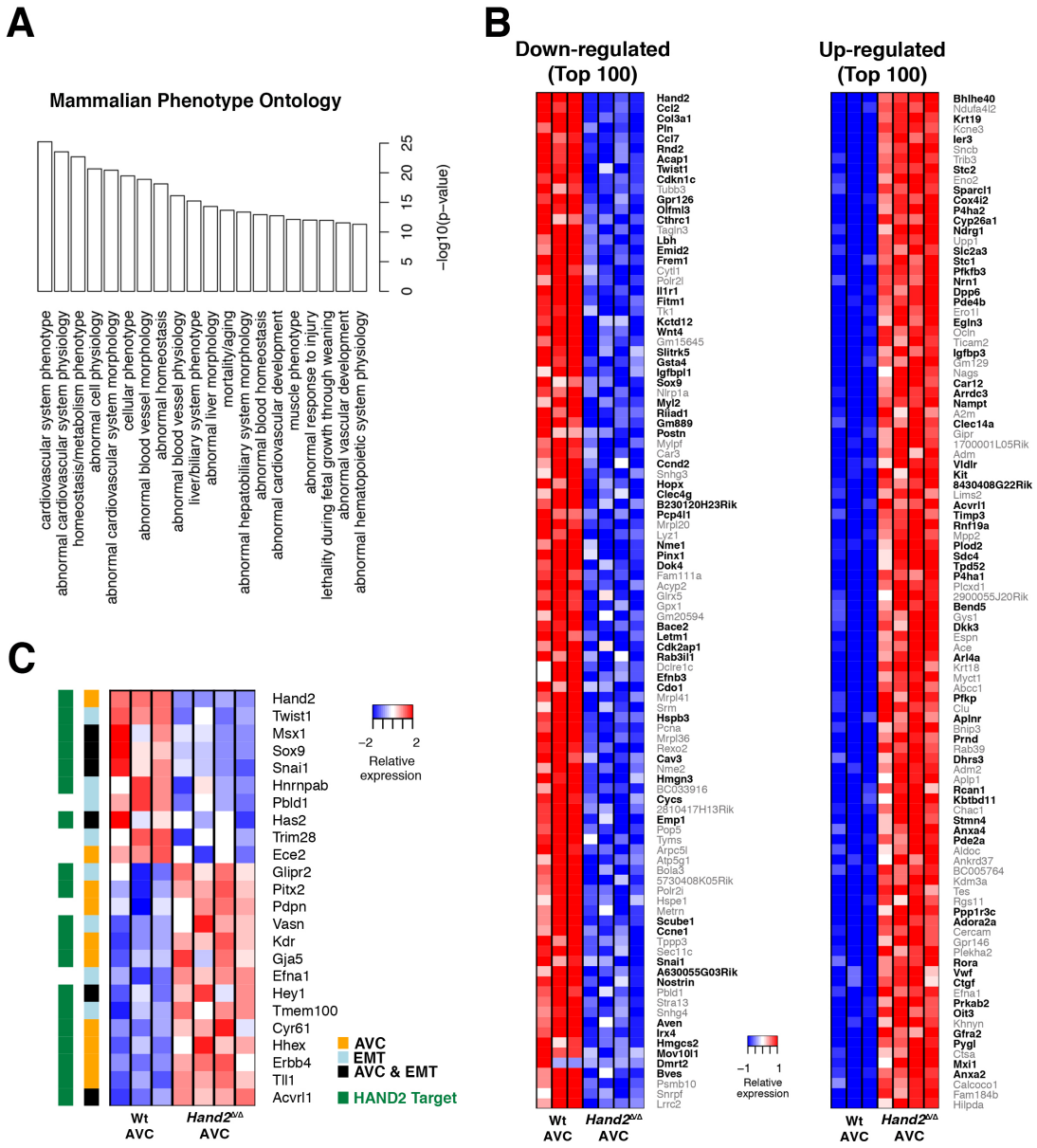

Figure S4 (related to Figure 4). Transcriptome analysis identifies the HAND2 target genes with significantly altered expression in *Hand2*-deficient AVCs.

(A) Enrichment analysis for mammalian phenotypes including all 1051 DEGs identified by comparative transcriptome analysis of *Hand2*$^{\Delta/\Delta}$ and wild-type AVCs. (B) Top 100 up- and down-regulated genes in *Hand2*-deficient AVCs in comparison to wild-type controls. Genes with regions enriched in HAND2 chromatin complexes within their TADs are indicated in bold black, others in grey. (C) Heat map of up- and down-regulated genes in *Hand2*-deficient AVCs annotated using the following gene ontology categories: MP:0000297 (abnormal AV cushion morphology + child terms) BP:0001837 (epithelial-mesenchymal transition) and BP:0010717 (regulation of EMT). Most of the DEGs in these categories are HAND2 target genes (indicated in green).

Figure S5

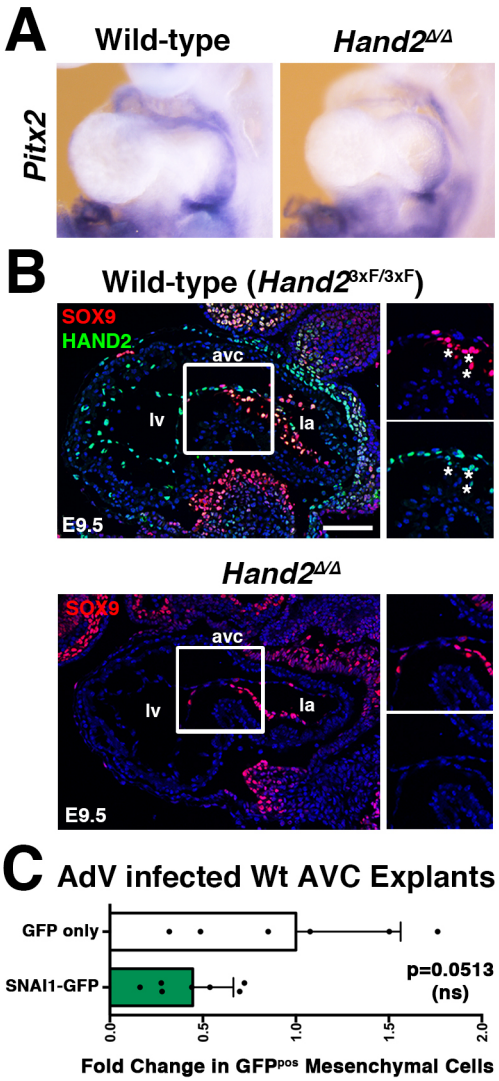

Figure S5 (related to Figures 5 and 6). Analysis of HAND2 target genes in the developing AVC.

(A) WISH analysis of the HAND2 target gene *Pitx2*, whose transcript levels are significantly altered in mutant AVCs by RNA-Seq analysis. No changes in the spatial distribution of *Pitx2* transcripts are detected. (B) Colocalization of HAND2^{3xF} proteins (green fluorescence) with the SOX9 transcriptional regulators (red fluorescence) in the AVC of wild-type (*Hand2*$^{3xF/3xF}$) and *Hand2*-deficient (*Hand2*$^{\Delta/\Delta}$) mouse embryos at E9.5. Asterisks in the enlargement (upper panels) point to SOX9-positive delaminating mesenchymal cells in the AVC, which are lacking in the *Hand2*-deficient AVC. Scale bar: 100µm. (C) Infection of wild-type AVC explants with GFP and SNAI1-GFP adenovirus (using 6x10^6 PFU for either virus per sample) indicates that GFP virus infects AVC cells slightly more efficiently than SNAI1-GFP virus. Therefore, the observed partial restoration of cell migration in *Hand2*-deficient AVCs infected with SNAI1-GFP virus is likely slightly underestimated (Figure 6B).

Figure S6

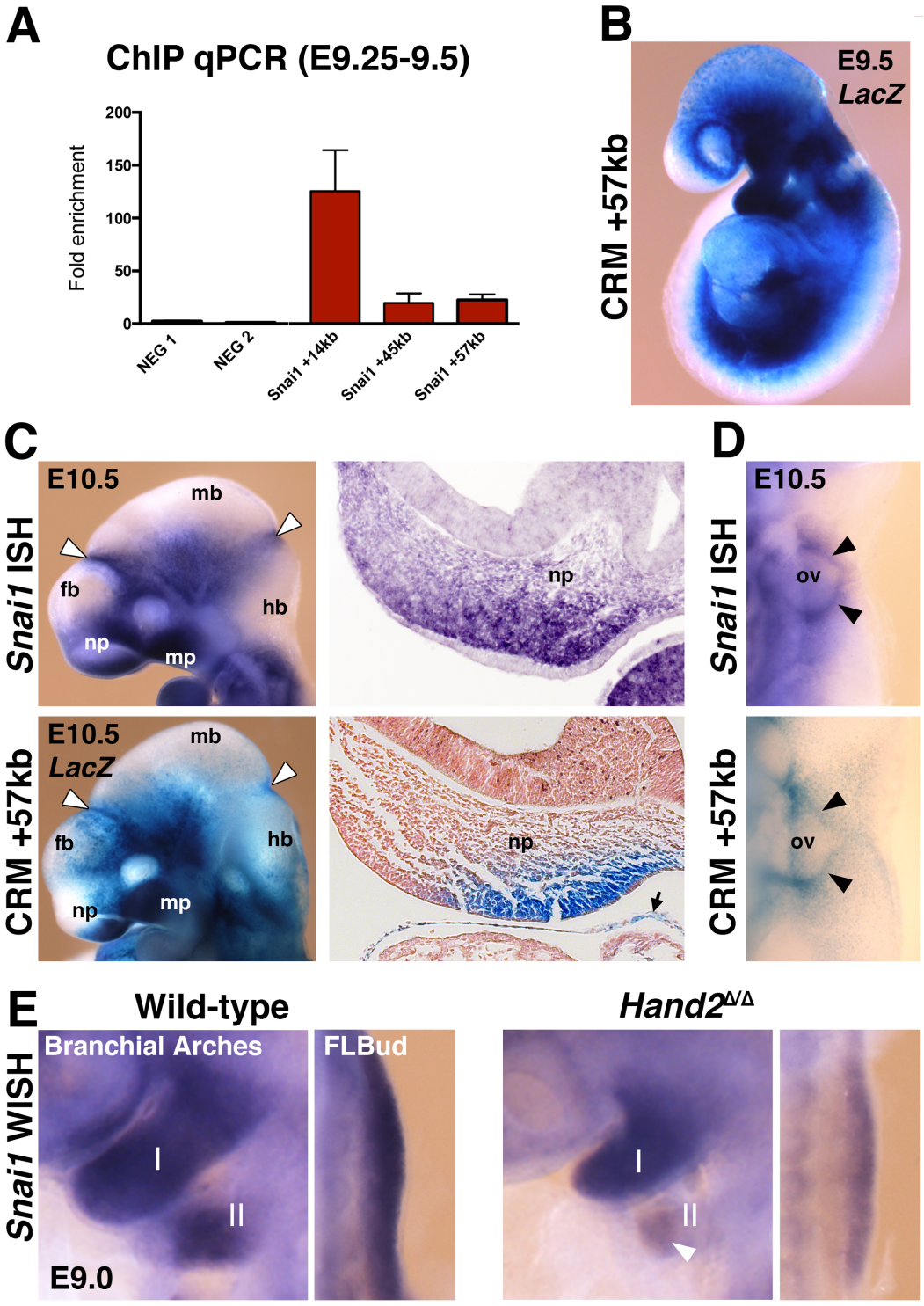

Figure S6 (related to Figure 6). The *Snai1* transcript distribution overlaps the CRM+57kb activity in craniofacial structures, branchial arches and early limb buds.

(A) ChIP-qPCR validation of the enrichment of the three CRMs in HAND2 chromatin complexes from embryonic hearts (E9.25-E9.5, n=2; mean ±SD). (B) The expression pattern of the *Snai1* CRM+57kb *LacZ* reporter transgene at E9.5. (C) *Snai1* expression and activity of the CRM+57kb *LacZ* reporter

transgene in craniofacial structures. The enhancer activity overlaps well with the domain of *Snai1* transcripts in the nasal prominence (np), maxillary process (mp), fore-midbrain and mid-hindbrain boundaries (white arrowheads). fb: forebrain, mb: midbrain, hb: hindbrain. Black arrow points to the epicardium. (D) Expression of *Snai1* and the CRM+57kb LacZ reporter transgene in migrating cardiac neural crest cells (black arrowheads) enveloping the otic vesicle (ov). (E) *Snai1* expression is reduced in the 2nd branchial arch (II) and early forelimb buds in *Hand2*-deficient mouse embryos (E9.0)

Supplemental Tables

Table S1 (related to Figure 1). List of the statistically validated HAND2 ChIP-Seq peaks in the dataset from mouse embryonic hearts (E10.5) and associated genes.

An Excel table of all peak IDs and coordinates (mm9) is included as a separate file (Supplemental Table S1).

GREAT was used to associate peaks to the nearest genes. Distances between the ChIP-Seq peak summit and the transcriptional start sites located within ≤1Mb are indicated. Peak ID is based on the decreasing value of the combined log2-enrichment from the two ChIP-Seq samples versus their inputs (MACS).

Table S2 (related to Figure 1). HAND2-enriched genomic regions associated to genes whose altered expression in *Hand2*-deficient mouse embryonic hearts have been published.

GREAT analysis revealed the association of HAND2 ChIP-Seq peaks with genes whose altered expression in *Hand2*-deficient hearts has been previously established by others (see references for details). For each gene, the numbers of genomic regions significantly enriched in HAND2 chromatin complexes in mouse embryonic hearts at E10.5 is indicated. The exact coordinates of the associated peaks are listed in Table S1, which is an Excel table that can be easily searched by gene name.

Gene	No. of ChIP-Seq Peaks	Reference
Adam19	1	(Holler et al., 2010)
Ankrd6	5	Holler et al., 2010
Anxa6	1	Holler et al., 2010
Armc9	1	(Tsuchihashi et al., 2011)
Bin1	4	Tsuchihashi et al., 2011
Bmp5	3	Tsuchihashi et al., 2011
Brp44l	1	Tsuchihashi et al., 2011
Cad	1	Tsuchihashi et al., 2011
Camk2a	1	Holler et al., 2010
Cdk6	4	Holler et al., 2010
Clasp2	1	Holler et al., 2010
Col11a1	1	Holler et al., 2010
Dll4	1	(VanDusen et al., 2014)
Ece1	4	Tsuchihashi et al., 2011
EfnB2	5	Van Dusen et al., 2014
Eid3	2	Tsuchihashi et al., 2011
Foxc1	9	Holler et al., 2010
Foxp2	1	Holler et al., 2010
Gata4	5	Tsuchihashi et al., 2011; (Srivastava et al., 1997)
Gja5	6	Holler et al., 2010; (McFadden et al., 2005)
Gli3	5	Holler et al., 2010
Has2	9	Tsuchihashi et al., 2011
Hey1	7	Holler et al., 2010
Hspa8	1	Tsuchihashi et al., 2011
Insm1	2	Holler et al., 2010
Irx4	3	(Bruneau et al., 2000)
Itga9	6	Holler et al., 2010
Klf4	4	Tsuchihashi et al., 2011
Lgi2	3	Tsuchihashi et al., 2011
Ltbp1	11	Holler et al., 2010
Lyve1	1	Van Dusen et al., 2014
Nav1	10	Holler et al., 2010
Nebl	9	Villanueva et al., 2002
Nrg1	7	Van Dusen et al., 2014
Nrip1	1	Tsuchihashi et al., 2011
Nrp1	9	Van Dusen et al., 2014

Pank1	1	Tsuchihashi et al., 2011
Pard3	15	Holler et al., 2010
Parp1	3	Tsuchihashi et al., 2011
Pdgrfa	3	(Barnes et al., 2011)
Peli1	5	Tsuchihashi et al., 2011
Plxna2	8	(Morikawa and Cserjesi, 2008)
Postn	2	Barnes et al., 2011
Rbm26	3	Tsuchihashi et al., 2011
Slc39a10	4	Tsuchihashi et al., 2011
Slc45a1	8	Tsuchihashi et al., 2011
Snrpd3	1	Tsuchihashi et al., 2011
Sox11	13	Holler et al., 2010
Stat5b	1	Holler et al., 2010
Syne1	6	Tsuchihashi et al., 2011
Tgif2	1	Holler et al., 2010
Tmem164	3	Tsuchihashi et al., 2011
Tmem87b	2	Tsuchihashi et al., 2011
Tor1aip1	1	Tsuchihashi et al., 2011
Vegfa	3	Van Dusen et al., 2014
Zfp516	12	Tsuchihashi et al., 2011

Table S3 (related to Figure 1 and S2). HAND2 ChIP-Seq peaks overlapping VISTA enhancers active in mouse embryonic hearts.

The peak ID is based on MACS enrichment. Distances from the ChIP-Seq peak summit to the transcriptional start sites of the neighboring genes are indicated.

Peak ID	Coordinates (mm9)			VISTA CRM		Gene 1	Distance (kb)	Gene 2	Distance (kb)
1	chr10	44949251	44950666	mm87		*Popdc3*	-59152	*Prep*	+162937
12	chr17	12982708	12984914	mm89		*Igf2r*	-21281	*Mas1*	+77198
19	chr3	151967094	151968437	mm72		*Nexn*	-38482	*Fam73a*	+35605
20	chr4	13759583	13760910	hs1658		*Runx1t1*	+89664	*Slc26a7*	+788705
64	chr3	104402785	104404252	mm143	hs1672	*Lrig2*	-87740	*Slc16a1*	-39072
121	chr5	93056454	93057879	mm187		*Stbd1*	+25090	*Ccdc158*	+46984
129	chr18	80525766	80528682	mm152		*Kcng2*	-34152	*Ctdp1*	+139210
155	chr5	150122171	150124072	hs1515		*Medag*	-91202	*Alox5ap*	+46488
167	chr11	11861513	11862778	mm178		*Ddc*	-64099	*Grb10*	+75258
196	chr13	46665895	46668189	mm132	hs1661	*C78339*	-97849	*Cap2*	+69825
217	chr12	80635258	80636662	hs1392		*Rad51b*	+234409	*Zfp36l1*	+578040
269	chr11	65021000	65023882	mm67		*Arhgap44*	-45978	*Myocd*	+61002
344	chr3	20045122	20046194	mm86		*Gyg*	+9558	*Hltf*	+87847
353	chr10	30772605	30773747	mm763		*Hey2*	-210569	*Gm5422*	-194815
368	chr8	97950228	97951513	mm71		*Gtl3*	+7898	*Mmp15*	+74703
413	chr3	137447812	137448973	mm4		*H2afz*	-79058	*Ddit4l*	+161757
448	chr5	132704995	132706570	mm131	hs1660	*Wbscr17*	-921995	*Auts2*	+311910
453	chr7	87589003	87591609	mm169		*Furin*	-42658	*Blm*	+89699
524	chr8	28216047	28218609	mm136	hs1665	*Gpr124*	+21015	*Brf2*	+21776
634	chr9	24778152	24779709	hs463		*Tbx20*	-200185	*Gm10181*	-114935
656	chr4	120064659	120066408	mm145	hs1674	*Foxo6*	-105580	*Scmh1*	-54218
757	chr12	84173003	84175084	mm78		*Rgs6*	+87746	*Dpf3*	+277838
834	chr9	24692274	24693500	mm130	hs1659	*Gm10181*	-200979	*Tbx20*	-114141
962	chr4	94984035	94985383	mm308	hs1485	*Jun*	-265796	*Fggy*	-239489
1263	chr10	39378652	39380031	hs1690		*Rev3l*	-72582	*Traf3ip2*	+46602
1290	chr14	55615136	55616687	mm771	hs1670	*Myh7*	-2441		
1383	chr7	75156457	75157757	hs1932		*Igf1r*	+59394	*Pgpep1l*	+252012
1436	chr5	77558679	77560618	mm770		*Hopx*	-15463	*Spink2*	+80847
1518	chr17	35856079	35859456	mm90		*Ier3*	-100861	*Ddr1*	-20213
1531	chr8	80511878	80513042	mm172		*Ednra*	-264125	*Ttc29*	-224781
1541	chr14	63678867	63681757	mm244		*Ctsb*	-60990	*Defb42*	+14484
1835	chr15	83466745	83472118	mm84		*Ttll12*	-43845	*Scube1*	+86019
1954	chr4	133285123	133286525	hs569		*Pigv*	-57262	*Arid1a*	+23702
2191	chr2	113948688	113949705	mm182		*Actc1*	-70574	*Aqr*	+51878
2219	chr8	35015890	35017195	mm70		*Rbpms*	+23770	*Gtf2e2*	+174157
2465	chr17	73371361	73372925	mm82		*Lclat1*	-85191	*Lbh*	+104498
2486	chr12	86776513	86777917	hs1657		*Tmed10*	-61548	*Fos*	-37625
3190	chr18	61810650	61815847	hs1752		*Il17b*	-34340	*Csnk1a1*	+98321
3236	chr6	72164733	72167870	mm123	hs1652	*Atoh8*	+19269	*St3gal5*	+118695
3596	chr10	56700222	56701185	mm74		*Hsf2*	-505487	*Gm9956*	+235764
3662	chr18	11371587	11374309	mm138	hs1667	*Rbbp8*	-418837	*Gata6*	+320440
3757	chr11	65461505	65462818	mm85		*Myocd*	-378719	*Map2k4*	+139637
3928	chr10	30948623	30949641	mm762		*Hey2*	-386525	*Gm5422*	-18859
4335	chr13	42353478	42354514	mm235		*Edn1*	-42643	*Hivep1*	+206606
4422	chr5	122542160	122545553	mm77		*Cux2*	-43997	*Myl2*	-7103
5216	chr11	77236747	77237741	mm146	hs1675	*Coro6*	-40169	*Ssh2*	+207455
5317	chr17	7471879	7478563	mm108		*Tcp10a*	-53814	*Rps6ka2*	+100757
5334	chr7	150296444	150299172	mm183		*Kcnq1*	+4649	*Cdkn1c*	+349147
5435	chr2	59666469	59670298	mm282		*Wdsub1*	+52257	*Tanc1*	+218283
5450	chr12	86795520	86797109	mm260	hs1481	*Tmed10*	-80648	*Fos*	-18525
5616	chr10	80234668	80240792	mm200		*Sf3a2*	-23213	*Dot1l*	+19779
5624	chr4	118690811	118693030	mm165		*Slc2a1*	-89395	*Lao1*	+57738
5905	chr9	47183420	47185651	mm251		*Cadm1*	-153804		
7081	chr19	53790405	53792424	mm64		*Pdcd4*	-175306	*Rbm20*	+39619
7605	chr13	73435705	73437570	mm68		*Gm10263*	-18664	*Irx4*	+38693
7892	chr19	40542066	40543214	hs2353		*Pdlim1*	-196534	*Sorbs1*	+45629
7898	chr8	123693474	123697140	mm241		*Foxc2*	+55236	*1700018B08Rik*	+370547
7946	chr12	12185772	12187084	mm103		*Fam49a*	-82517	*Rad51ap2*	+723543
8076	chr4	153766741	153769146	hs1912		*Arhgef16*	-93781	*Prdm16*	+243031
8149	chr1	92876838	92877812	hs1945		*Lrrfip1*	-72696	*Rab17*	-11087
8200	chr11	46015056	46016378	mm102		*Nipal4*	-35707	*Fndc9*	-33316
9393	chr17	12985103	12986168	mm89		*Igf2r*	-23106	*Mas1*	+75373
9430	chr14	63986052	63989651	mm245		*Gata4*	-123744	*Blk*	+48172
9473	chr18	14055424	14056614	hs369		*Zfp521*	+75223	*Hrh4*	+890520
9792	chr5	38900176	38902270	mm253		*Slc2a9*	-29678	*Wdr1*	+51682
10090	chr9	63891864	63893712	mm69		*Lctl*	-72166	*Smad6*	-22922
10093	chr18	11077550	11078792	hs502		*Rbbp8*	-713614	*Gata6*	+25663
10172	chr1	39499627	39501386	hs1933		*Tbc1d8*	+35085	*Rpl31*	+75811
10217	chr14	26403212	26409922	hs1767		*Ppif*	-107089	*Zmiz1*	+127857
10492	chr17	49829797	49831340	mm276		*Kif6*	+76072	*Rftn1*	+499430
11712	chr10	30717765	30718810	mm766		*Gm5422*	-249703	*Hey2*	-155681

Table S4 (related to Figures 1 and S3). HAND2 target genes annotated to GO terms relevant for outflow tract and right ventricle development.

The expression of genes highlighted was comparatively analyzed in wild-type and *Hand2*-deficient embryos.

Outflow tract HAND2 target genes (n=43) BP:0003151: outflow tract morphogenesis MP:0006126: abnormal outflow tract development	**Right ventricle HAND2 target genes (n=105)** BP:0003205: cardiac chamber development MP:0003920: abnormal heart right ventricle morphology		**OFT and RV shared HAND2 target genes (n=59)**
Aldh1a2	*Abca1*	*Mef2a*	*Acvr1*
Ate1	*Adam12*	*Myh10*	*Adam19*
Atf2	*Adamts1*	*Myh7*	*Bmp10*
Bmpr1a	*Adora2a*	*Myl2*	*Bmp4*
Cdh5	*Adra2b*	*Myl3*	*Cc2d2a*
Dicer1	*Ahr*	*Mylk3*	*Chrd*
Ece1	*Ank2*	*Myocd*	*Cited2*
Ednra	*Arid1a*	*Myoz2*	*Cxcr7*
Eng	*Atp2a2*	*Ngf*	*Fgf10*
Eya1	*Bmpr2*	*Notch1*	*Fgfr2*
Fbln1	*Btc*	*Notch2*	*Foxc2*
Fn1	*Cacna1c*	*Nphp3*	*Fzd1*
Foxp1	*Cav3*	*Npr1*	*Gata4*
Irx3	*Cdh2*	*Opa3*	*Gata5*
Irx5	*Cep110*	*Ovol2*	*Gata6*
Jun	*Col11a1*	*Pdgfb*	*Gja1*
Kcnh2	*Cpe*	*Pdlim3*	*Gja5*
Ltbp1	*Cxcr4*	*Pdpk1*	*Hand1*
Map2k5	*Cyr61*	*Pkp2*	*Hand2*
Meox2	*Dand5*	*Pla2g4a*	*Has2*
Mkl1	*Des*	*Plce1*	*Hes1*
Mkl2	*Dll4*	*Pou4f1*	*Hey1*
Nedd4	*Dnahc11*	*Pparg*	*Hey2*
Nipbl	*Dnaja3*	*Prox1*	*Heyl*
Nrp2	*Dock1*	*Ramp2*	*Hhex*
Nxn	*Dsp*	*Rbm15*	*Hif1a*
Pcsk5	*Edn1*	*Robo1*	*Hoxa1*
Pdgfra	*Efnb2*	*Ryr2*	*Isl1*
Pds5a	*Egfr*	*Sall1*	*Jag1*
Pds5b	*Egln1*	*Scn5a*	*Mef2c*
Plxnd1	*Erbb4*	*Sema3a*	*Mesp1*
Rarb	*Fbln5*	*Shox2*	*Msx2*
Rdh10	*Fbn1*	*Slco2a1*	*Nfatc1*
Sec24b	*Fgf9*	*Slit3*	*Nkx2-5*
Shh	*Fgfr1*	*Smad7*	*Ntf3*
Six1	*Fgfrl1*	*Smarca4*	*Ntrk3*
Snai1	*Fhl2*	*Smarcd3*	*Parva*
Sox17	*Foxc1*	*Srf*	*Pdgfrb*
Tfap2a	*Foxf1*	*Tbx5*	*Phc1*
Tgfbr2	*Frs2*	*Tek*	*Pitx2*
Thbs1	*Gab1*	*Thbd*	*Ptpn11*
Twist1	*Gata3*	*Timp4*	*Rbpj*
Vegfa	*Gsk3a*	*Tnni1*	*Rxra*
	Gucy1a3	*Tnnt2*	*Sfrp2*
	Hdac2	*Tpm1*	*Smad6*
	Hectd1	*Wnt2*	*Sox11*
	Heg1		*Sox4*
	Hmox1		*Tbx1*
	Id2		*Tbx2*
	Ift88		*Tbx20*
	Igf2		*Tbx3*
	Igf2r		*Tdg*
	Itgb1		*Tgfb2*
	Jup		*Tgfbr3*
	Ldb3		*Vangl2*
	Lefty2		*Vcan*
	Lmna		*Wnt11*
	Lmo4		*Wnt5a*
	Luzp1		*Zfpm2*

Table S5 (related to Figure 4 and S4). Comparative transcriptome analysis of the genes expressed in wild-type and *Hand2*-deficient AVCs (E9.25-E9.5).

An Excel table of all expressed genes is included as a separate file (Supplemental Table S5).

In addition to the gene names the following parameters are shown. log2 FC: log2 fold change in normalized expression levels between wild-type (n=3) and mutant AVC transcriptomes (n=4). PValue: p-value indicating statistical significance of the observed differences. FDR: false discovery rate (given as E = exponential value). Expression in *Hand2* mut: indicates if transcript levels in the *Hand2*-deficient AVC samples (compared to wild-type AVC) are reduced (DOWN), unchanged (UNCHANGED) or increased (UP). HAND2 ChIP Peak: YES indicates that the gene is associated with regions enriched by HAND2 ChIP-Seq analysis, NO: no associated HAND2 ChIP-Seq peaks. In addition to the list of all expressed genes, lists showing all significantly up-regulated (up_reg_genes) and down-regulated genes (down_reg_genes) are also included.

Table S6 (related to Figures 4D, 5, 6 and S5). Difference in expression levels of HAND2 target genes with functions in EMT and/or AVC cardiac cushion development

This table lists the actual values for all HAND2 target genes in the AVC shown in Figure 4D and analyzed in Figures 5,6 and S5. RPM: reads per million sequenced reads; log2 FC: log2 fold change; linear FC: linear fold change; p-Value: statistical significance, indicated as exponential value; FPR: false discovery rate, indicated as exponential value; DEG: differentially expressed gene; DOWN: reduced transcript levels in mutant AVC samples; UP: increased transcript levels in mutant AVC samples

	RPM mutant AVC samples				RPM wt AVC samples							
Gene	**1**	**2**	**3**	**4**	**1**	**2**	**3**	**log2 FC**	**linear FC**	**p-Value**	**FDR**	**DEG**
Hand2	0.19	0.82	0.36	0.37	49.14	44.00	44.47	-6.73	-106.38	6.85E-114	7.66E-110	DOWN
Twist1	4.51	3.67	8.09	3.10	20.25	17.33	24.06	-2.09	-4.26	2.44E-12	3.92E-10	DOWN
Msx1	1.20	1.11	1.71	1.79	3.80	1.83	6.29	-1.46	-2.74	5.48E-04	9.10E-03	DOWN
Sox9	46.09	43.27	55.95	57.36	93.61	78.65	192.27	-1.27	-2.41	5.85E-07	3.22E-05	DOWN
Snai1	3.01	3.67	4.90	5.32	9.44	7.30	13.00	-1.24	-2.36	2.70E-05	8.15E-04	DOWN
Hnrnpab	185.57	198.29	285.61	143.13	371.12	469.47	269.96	-0.88	-1.84	1.23E-04	2.94E-03	DOWN
Has2	40.33	66.56	53.01	72.78	79.40	63.62	145.37	-0.74	-1.67	4.63E-03	4.16E-02	DOWN
Glipr2	187.54	236.90	184.96	234.11	121.92	102.84	182.02	0.62	1.54	2.13E-03	2.47E-02	UP
Pitx2	56.68	70.23	60.05	60.54	42.50	33.32	43.39	0.62	1.54	3.41E-04	6.33E-03	UP
Vasn	11.64	12.25	15.89	9.60	7.89	7.48	6.33	0.76	1.69	1.73E-03	2.14E-02	UP
Kdr	88.01	116.98	85.33	89.83	54.56	52.30	39.44	0.94	1.92	3.75E-07	2.15E-05	UP
Gja5	58.12	81.82	36.79	101.62	36.97	36.30	25.25	1.06	2.08	1.87E-04	4.01E-03	UP
Hey1	50.94	27.98	64.33	42.07	19.44	27.82	17.28	1.10	2.15	2.93E-05	8.66E-04	UP
Tmem100	31.55	30.70	20.79	35.23	14.79	16.14	9.27	1.12	2.18	4.35E-06	1.70E-04	UP
Cyr61	56.34	159.33	89.76	83.69	47.08	36.20	39.37	1.23	2.34	9.77E-06	3.43E-04	UP
Hhex	14.37	12.28	21.73	9.38	5.37	7.15	4.88	1.31	2.48	9.42E-06	3.37E-04	UP
Erbb4	3.62	6.93	6.39	5.00	2.27	2.05	2.20	1.31	2.49	1.07E-04	2.61E-03	UP
Tll1	3.17	4.68	3.41	4.20	0.62	1.11	0.63	2.28	4.84	9.30E-09	7.65E-07	UP
Acvrl1	12.53	8.93	7.44	11.57	2.31	1.62	1.01	2.59	6.02	3.48E-14	8.46E-12	UP

Supplemental Experimental Procedures

ChIP-Seq peak-calling and data analysis

The number of reads sequenced/aligned per ChIP-Seq sample were as follows:

Sample	No. of reads sequenced	No. of reads mapped to the genome
Replicate A (ChIP)	139,781,750	112,355,481
Replicate A (input)	60,489,198	46,937,735
Replicate B (ChIP)	102,690,152	70,308,925
Replicate B (input)	67,745,942	51,072,733

Reads were mapped to the mouse genome (NCBI37/mm9) using the qAlign function from QuasR (Gaidatzis et al., 2015) package with default parameters, except that up to 10 hits in the genome were allowed. The sample specific fragment sizes were estimated from cross correlation profiles of read density on both chromosomal strands using the Chipcor software (http://ccg.vital-it.ch/chipseq). Reads were shifted by half of the fragment size (100bp) towards the middle of the fragment. Peaks were detected using MACS (Zhang et al., 2008) (version 1.4.2, with parameters --tsize=50 --pvalue=1e-5 --mfold=10,30 --nomodel --shiftsize=100 –keep-dup=1) for the pooled replicates of ChIP samples in combination with pooled input controls. Peaks were sorted based on the enrichment over the input control samples. ChIP enrichment of each peak was calculated as e = log2((n_fg /N_fg *min(N_fg,N_bg) + p) / (n_bg /N_bg *min(N_fg,N_bg) + p)), where n_fg and n_bg are the summed weights of overlapping foreground and background (input chromatin) read alignments, respectively. N_fg and N_bg are the total number of aligned reads in foreground and background samples, and p is a pseudo-count constant (p=8) used to minimize the sampling noise for peaks with very low counts. The read counts in the peaks called on the pooled samples were then re-quantified separately on the two replicates. As an indication of the high reproducibility of the inferred maps of HAND2-binding sites,

the log2-transformed counts showed a Pearson's correlation coefficient of 0.63 between replicates. The fraction of reads under the peaks (FRiP) (Landt et al., 2012) for the two independent ChIP-Seq samples was 3.15% and 6.66%, respectively. This is well above of the value of FRiP that was considered as acceptable (1%) by the ENCODE consortium (Landt et al., 2012), which underscores the high signal-to-noise ratio in both ChIP-Seq samples. HAND2-interacting genomic regions were associated to their neighboring genes using the "basal plus extension" domain (≤1Mb) from GREAT version 3.0.0 (McLean et al., 2010).

Functional enrichment analysis

The 12117 HAND2-enriched peaks identified by ChIP-Seq were sorted by the combined enrichment values over the two replicates and split into deciles. GREAT was then run on the first deciles, the pool of the first two deciles and so on by incrementally pooling the subsequent deciles up to reconstituting the complete list of HAND2 peaks. The terms for mouse phenotypes from MGI (Bult et al., 2008) and the Gene Ontology (GO) terms for biological processes were used (Ashburner et al., 2000). Specific heart-related terms were manually extracted (using the following keywords/patterns: heart, card-, ventric-, cushion, atria, atrium, atrioventricular, septum, trabec-, endoc-, myoc-, coronary, outflow, valve, tricuspid, conduction) and those showing statistically significant enrichment were retained. In order to be considered, each term must show a FDR ≤1e-5 (hyper-geometric test) in at least two out of the ten incremental bins considered. FDRs were log10-transformed and their sign inverted. These numbers were then hierarchically clustered (Euclidean distance, complete linkage); the dendrogram was finally re-ordered according to the mean of these values across the ten bins using the reorder function of R. Fig 1C shows the 16 highest enriched GO terms from the whole cistrome, but the direct ontological child

term of some of these terms are not shown due to redundant annotations between development-related terms and their direct morphogenesis-related child terms.

Analysis of Evolutionary Conservation

To calculate the evolutionary conservation of HAND2-interacting genomic regions, the average PhastCons conservation score for a subset of 11 species (euarchontoglires) was calculated for each base within the ±1500bp surrounding each peak summit.

***De novo* motif discovery**

The findMotifsGenome.pl script in the HOMER collection (Heinz et al., 2010) was used to perform: 1. over-representation analysis of known TF-binding sites and 2. *de novo* motif discovery using a fixed length of 7 nucleotides. The region ±150 bps surrounding the summit of each peak was considered. The 20 most over-represented matrices for the top 5 motifs highlighted by *de novo* motif discovery were then used to scan the region for high-affinity matches using FIMO (Grant et al., 2011). The p-value threshold to report a hit was set to 1e-4. Only the matrices obtained from mammalian datasets and showing at least one high-affinity match across the HAND2 ChIP-Seq peaks were retained. The resulting list of matches was transformed to a matrix with the motifs on the rows and the regions on the columns. P-values were log10-transformed and their sign inverted, then hierarchically clustered (Euclidean distance, complete linkage).

Hierarchical clustering, plotting and statistical testing

Clustering, plots and statistics were performed using R.

ChIP-qPCR analysis

All genomic regions analyzed in more detail were verified by ChIP-qPCR using embryonic hearts (*Hand2*$^{3xF/3xF}$) at E9.25-E9.5 (n=2 biological replicates) and E10.5 (n=3 biological replicates). An unlinked amplicon targeting the *Actb* locus was used as normalizing control and to calculate the fold-enrichment. To prevent artefactual bias of fold enrichments, a cycle threshold of 32 was defined as background. For each experiment, two genomic regions not enriched in the HAND2 ChIP-Seq dataset were used as negative controls. The oligos used for qPCR amplification are listed here.

ChIP Amplicon	Forward primer	Reverse primer
Actb +1.8kb control	5'GATCTGAGACATGCAAGGAGTG3'	5'GGCCTTGGAGTGTGTATTGAG3'
NEG 1 *Snai1* +64kb	5'CCACCTGTCTGCCCTTAGTC3'	5'GGGCTTCTTGAACTACC3'
NEG 2 *Furin* -50kb	5'CTACATGAGGGTTGGGGAGA-3'	5'TGCTCTGCTGATGGCTAAAA3'
Gata4 -124kb	5'CTTCTCGAAGGCAGCAGTCT-3'	5'GGACTGATGAGGTGGAAGGA3'
Myocd +60kb	5'TGGCTATTGTCCCTCCAGAC-3'	5'GGATGATGTCAGGGCTTCTC3'
Gata6 +320kb	5'GACGTTATCAAAGCTCCACATTC3'	5'AAAAGTCAGCTGTAAGCTCTTGG3'
Tbx20 -114kb	5'AGCCCTGGGTCTCTTCACTT3'	5'TGAGAGAAAGCAGAGCGGAG3'
Wnt11 +206kb	5'TTTTGGTATGAAGGACACGGA3'	5'CACAAGCGTTTGCCTAGATAACT3'
Wnt5a -378kb	5'GAAAGAGTGGATGTGTGTGTGAG3'	5'AGGCCCACTTCTCTGGTTAAT3'
Bmp4 -272kb	5'AAGCCACCCCACTGGTATTC3'	5'TAGTTCCCTTGCACAGCAGG3'
Tgfb2 +482kb	5'CCCATCACAGGAGTGAATGA3'	5'ACTTGACCTCTGCCATCTGC3'
Fgf10 -231kb	5'AATCCCCTTTCCGATCTGTC3'	5'ACTGGCTTCATGTCTTCCCA3'
Has2 -26kb	5'ATCCGTTGTGAAGCACTTGAG3'	5'GTCGCTTCACTTCATTGCTTC3'
Snai1 +14kb	5'GCTTTGCCTGTTCAGGACAT3'	5'GAAAGCACGGCCTATGAGAA3'
Snai1 +45kb	5'ACTCTCCGGGGACAGCTAATA3'	5'CCCACTGCTTTGATCAGCTT3'
Snai1 +57kb	5'TCTGCTGGCCTCCAGATGT3'	5'TTGATAAAGCCCCTCTGTGC3'
Hand2 +12kb	5'TCGCTTAGTCGCCTTCTCAT3'	5'GTTCTTTGCCCCAGATTTCC3'
Twist1 +10kb	5'CCTCTGGTTGACACAAAGCA3'	5'TGGGGACTAGGACACCAGAC3'
Msx1 -69kb	5'AATTCAGCGCTTGAACGTCT3'	5'CCACTTAGCAAACCGCAAAT3'
Sox9 +196kb	5'GATGGCTGGAACCACTGTCT3'	5'GGGGAGTGGGGTTATTTAGC3'
Hnrnapab +85kb	5'CCTCGCTGGTTGACTTTGAG3'	5'TGTCAGGATGTGCATGTGTG3'
Glipr2 -26kb	5'ACAGGGCCTAAAGCATCAAC3'	5'CCGTCTTGTCTCTGTGTGGA3'
Pitx2 +585kb	5'ACAAATGCCAGCCTCAGAAC3'	5'GATTTGCATCTCCTGCCCTA3'
Vasn +792kb	5'ACCTCCAATGATTCCACTGC3'	5'GAGCCACAGATTGTCACAGC3'
Kdr -30kb	5'ATCTAGCCCTCCCCAACCTA3'	5'TGACCTGGCTTTGTGAGTTG3'
Gja5 +31kb	5'TCAAAGGGAAACACCTCTGG3'	5'GGACAGATTGGCAGGGTCTA3'
Hey1 -45kb	5'AGGTGGATCAGATGGACAGC3'	5'GGAAAGCCTTGTGGACTCTG3'

Tmem100+99kb	5'AGGTCGTTCTCTCGTGCATT3'	5'AGCTCCTTGACAACCTCCAA3'
Cyr61 +6.8kb	5'TCCAAGAGCAATGTGACACC3'	5'GGAGTTTTGGGTGTGGTTA3'
Hhex +9kb	5'CAGCCACTGTGAGGTTTTCA3'	5'ATGGCCTCCTCCTTCTCCTA3'
Erbb4 +345kb	5'GCTCAGACCAATGGTTCGTT3'	5'ACACAACTGCGGATGTCAAG3'
Tll1 -14kb	5'GGTGAGGAATGCAATGGACT3'	5'TAAATCCCAGTGGTCGTTCC3'
Acvrl1 +35kb	5'CTCCAAATGGCGAACTTGAT3'	5'ACCATGGCAGATGTCACTCA3'

Transcriptome analysis

AVCs dissected from wild-type and *Hand2*$^{\Delta/\Delta}$ mouse embryos at E9.0-9.25 (18-23 somites) were flash frozen in RLT buffer (Qiagen). Four AVCs per replicate were pooled keeping the same gender and age ratio for all replicates. RNA was extracted using the QIAGEN RNeasy mini kit. The quality of total RNA (30-60ng) was analyzed using the Agilent 2100 Bioanalyzer. Only samples with a RIN ≥8.5 were use for library construction using the Clontech SMARTer kit and sequenced on Illumina HiSeq 3000 using a single-read 50-cycles protocol.

Single-end reads were aligned to the mm9 reference genome and to the *Mus Musculus* transcriptome (iGenome refGene GTF) using TopHat v2.0.13 (Kim et al., 2013). The parameters were left to default, except for using the option *--no-coverage-search*. Profiles for the UCSC genome browser (Fujita et al., 2011) were generated considering just reads with a unique mapping position on the genome. These reads were fished out from the bam files using the option *-q 1* of SAMtools (Li et al., 2009). Profiles were obtained using *genomeCoverageBed* from BedTools v2.17.0 and linearly re-scaled according to sequencing depth (RPM, Reads Per Million sequenced reads; (Quinlan and Hall, 2010). Gene-wise counts were calculated using *htseq-count* from the HTSeq package with *-s* set to *no* (Anders et al., 2015). Only uniquely mapped reads were considered. *edgeR* was used to assess differential expression (Robinson et al., 2010). Libraries were normalized according to TMM normalization. Tag-wise estimation of dispersion was evaluated using *prior.df =10*. Only those genes

showing expression (RPM ≥ 1) in at least three samples were considered for the differential analysis. This was evaluated using the *exactTest* function in R. False discovery rates were estimated using the Benjamini-Hochberg correction. Differentially expressed genes (DEGs) were defined as those showing a *q*-value ≤0.05 and a linear fold-change ≥1.5. R was used to run *edgeR* and to generate heat maps.

Functional annotation of differentially expressed genes (DEGs)

Functional enrichments were calculated using DAVID 6.8 and MouseMine; the latter was applied to specifically evaluate the enrichment in annotated mouse phenotypes (Huang da et al., 2009; Motenko et al., 2015). Lists of *Epithelial-to-Mesenchymal Transition* (EMT) and *Atrio-Ventricular Canal cushions morphogenesis* (AVC) were retrieved as follows. Genes annotated as GO:0001837 or GO:0010717 in AMIGO, were considered as involved in EMT (Carbon et al., 2009). Genes annotated as MP:0000297 (and children terms) in the MGI were considered as involved in AVC (Blake et al., 2017). These lists were retrieved from the indicated websites on January 23, 2017. HAND2-target genes associations were defined by GREAT v3.0.0, which was run with default parameters (McLean et al., 2010). EMT- and AVC-specific sets of HAND2-target genes were obtained by intersecting these lists with the DEGs and the annotations described in this paragraph.

Genomic regions used for generating *LacZ* reporter transgenic mouse embryos

CRM	ChIP-Seq peaks (NCBI37/mm9)	Region tested for *LacZ* activity (NCBI37/mm9)	Forward / Reverse primers	Size (bp)
Snai1 +14kb	chr2:167,376,621-167,379,511	chr2:167376492-167379526	5'-GGGAGACTGACGCAAGAGAC-3'	3035
			5'-CAAAGGTGGAGGGATCAAGA-3'	
Snai1 +45kb	*	chr2:167,408,344-167,409,540	5'-CGATGTTCTGAGAGCATCTTGA-3'	1197
			5'-CCCCATTCTGTCTAACTGCAA-3'	

Snai1 +57kb	chr2:167,418,460-167,423,821	chr2:167,419,933-167,424,557	isolated from BAC RP23-193B17 as HpaI/MfeI fragment	4625

*the *Snai1*+45kb peak was not called by MACS, but its significant enrichment in HAND2 chromatin complexes isolated from mouse embryonic hearts at E9.5 was established by ChIP-qPCR analysis (Figure S6A).

In situ hybridization probes

The following probes were kind gifts from A. Nieto: *Snai1*; J. Martin: *Has2* and *Tgfβ2*; S. Evans: *Wnt11;* A. Kispert: *Gata4* and *Hey2*; M. Parmacek: *Myocd* and S. Arnold and S. Probst: *Hhex*. All other probes were generated by RT-PCR amplification of published fragments that where cloned into the appropriate vectors encoding Sp6 and T7 RNA polymerase binding sites to generate antisense riboprobes.

Immunohistochemistry

Embryos were collected and fixed in 4% PFA overnight at 4°C prior to embedding in paraffin. Sections were rehydrated and antigens retrieved by heating them for 5 min at 120°C in 10mM Sodium Citrate (pH 6.0) containing 0.05% Tween-20. Sections were incubated overnight at 4°C with primary antibodies detecting the following epitopes: FLAG (M2; 1:500; Sigma F1804), KI67 (1:200; Millipore ab9260), SMA-Cy3 (1:250; Sigma C6198), SOX9 (1:5000, Millipore ab5535). Alternatively, embryos were fixed in 4% PFA for 2hrs at 4°C, embedded in a 1:1 mixture of 30% Sucrose and OCT and frozen at -80OC. Cryosections were used in combination with the following primary antibody: PECAM-647 (1:200; Biolegend 102515). Sections were incubated with either goat anti-mouse (FLAG), goat anti-rabbit (KI67) secondary antibodies conjugated to Alexa Fluor 488 or 594 (1:1000, Life Technologies) for 1 hour at room temperature. For detecting two antigens simultaneously, the anti-FLAG M2 antibody was directly labeled using the APEX™ Alexa Fluor® 488 Antibody Labeling Kit (Life Technologies). Immunostaining was performed as follows:

overnight incubation with mouse primary antibody (anti-TWIST1: 1:500, Santa Cruz sc81417) was followed by a one-hour incubation with goat anti-mouse Alexa 594. Then sections were incubated again overnight with Alexa 488-labelled anti-FLAG M2. The next day, they were incubated for 1hour with rabbit anti-Alexa488 and finally for 1 hour with goat anti-rabbit Alexa 488 to enhance the signal. Nuclei were counterstained with Hoechst-33258. Images were acquired using a Leica SP5 confocal microscope.

AVC explant cultures

The matrix for AVC explant cultures (Luna-Zurita et al., 2010) was prepared by distributing a 1.5mg/ml solution of rat-tail collagen-type I in M199 medium (Life Technologies) in 24-well plates. This matrix was allowed to solidify for 1hr at 37°C in 5%CO2. Following 4-5 washes in M199 medium (30min each), the collagen matrixes were incubated for ≥1hr in M199 medium supplemented with 1% FBS, 1% L-Glutamine, 0.1% insulin-transferrin-selenium (ITS, Life Technologies) and antibiotics. AVC explants from E9.5 embryonic hearts were carefully dissected in ice-cold PBS, cut open and placed with the endocardium facing down onto the collagen matrixes after removing the excess medium. Following placement, the explants were left to attach for 4-5hrs at 37°C in 5%CO2. Complete M199 medium (150µl/well) was added and explants were cultured for 3 days.

Supplemental References

Anders, S., Pyl, P.T., and Huber, W. (2015). HTSeq-a Python framework to work with high-throughput sequencing data. Bioinformatics *31*, 166-169.

Ashburner, M., Ball, C.A., Blake, J.A., Botstein, D., Butler, H., Cherry, J.M., Davis, A.P., Dolinski, K., Dwight, S.S., Eppig, J.T.*, et al.* (2000). Gene ontology: tool for the unification of biology. The Gene Ontology Consortium. Nat Genet *25*, 25-29.

Barnes, R.M., Firulli, B.A., VanDusen, N.J., Morikawa, Y., Conway, S.J., Cserjesi, P., Vincentz, J.W., and Firulli, A.B. (2011). Hand2 loss-of-function in Hand1-expressing cells reveals distinct roles in epicardial and coronary vessel development. Circ Res *108*, 940-949.

Blake, J.A., Eppig, J.T., Kadin, J.A., Richardson, J.E., Smith, C.L., Bult, C.J., and the Mouse Genome Database, G. (2017). Mouse Genome Database (MGD)-2017: community knowledge resource for the laboratory mouse. Nucleic Acids Res *45*, D723-D729.

Bruneau, B.G., Bao, Z.Z., Tanaka, M., Schott, J.J., Izumo, S., Cepko, C.L., Seidman, J.G., and Seidman, C.E. (2000). Cardiac expression of the ventricle-specific homeobox gene Irx4 is modulated by Nkx2-5 and dHand. Dev Biol *217*, 266-277.

Bult, C.J., Eppig, J.T., Kadin, J.A., Richardson, J.E., Blake, J.A., and Mouse Genome Database, G. (2008). The Mouse Genome Database (MGD): mouse biology and model systems. Nucleic Acids Res *36*, D724-728.

Carbon, S., Ireland, A., Mungall, C.J., Shu, S., Marshall, B., Lewis, S., Ami, G.O.H., and Web Presence Working, G. (2009). AmiGO: online access to ontology and annotation data. Bioinformatics *25*, 288-289.

Fujita, P.A., Rhead, B., Zweig, A.S., Hinrichs, A.S., Karolchik, D., Cline, M.S., Goldman, M., Barber, G.P., Clawson, H., Coelho, A.*, et al.* (2011). The UCSC Genome Browser database: update 2011. Nucleic Acids Res *39*, D876-882.

Gaidatzis, D., Lerch, A., Hahne, F., and Stadler, M.B. (2015). QuasR: quantification and annotation of short reads in R. Bioinformatics *31*, 1130-1132.

Grant, C.E., Bailey, T.L., and Noble, W.S. (2011). FIMO: scanning for occurrences of a given motif. Bioinformatics *27*, 1017-1018.

Heinz, S., Benner, C., Spann, N., Bertolino, E., Lin, Y.C., Laslo, P., Cheng, J.X., Murre, C., Singh, H., and Glass, C.K. (2010). Simple combinations of lineage-determining transcription factors prime cis-regulatory elements required for macrophage and B cell identities. Mol Cell *38*, 576-589.

Holler, K.L., Hendershot, T.J., Troy, S.E., Vincentz, J.W., Firulli, A.B., and Howard, M.J. (2010). Targeted deletion of Hand2 in cardiac neural crest-derived cells influences cardiac gene expression and outflow tract development. Dev Biol *341*, 291-304.

Huang da, W., Sherman, B.T., and Lempicki, R.A. (2009). Systematic and integrative analysis of large gene lists using DAVID bioinformatics resources. Nat Protoc *4*, 44-57.

Kim, D., Pertea, G., Trapnell, C., Pimentel, H., Kelley, R., and Salzberg, S.L. (2013). TopHat2: accurate alignment of transcriptomes in the presence of insertions, deletions and gene fusions. Genome Biol *14*, R36.

Landt, S.G., Marinov, G.K., Kundaje, A., Kheradpour, P., Pauli, F., Batzoglou, S., Bernstein, B.E., Bickel, P., Brown, J.B., Cayting, P.*, et al.* (2012). ChIP-seq guidelines and practices of the ENCODE and modENCODE consortia. Genome Res *22*, 1813-1831.

Li, H., Handsaker, B., Wysoker, A., Fennell, T., Ruan, J., Homer, N., Marth, G., Abecasis, G., Durbin, R., and Genome Project Data Processing, S. (2009). The Sequence Alignment/Map format and SAMtools. Bioinformatics *25*, 2078-2079.

Luna-Zurita, L., Prados, B., Grego-Bessa, J., Luxan, G., del Monte, G., Benguria, A., Adams, R.H., Perez-Pomares, J.M., and de la Pompa, J.L. (2010). Integration of a Notch-dependent mesenchymal gene program and Bmp2-driven cell invasiveness regulates murine cardiac valve formation. J Clin Invest *120*, 3493-3507.

McFadden, D.G., Barbosa, A.C., Richardson, J.A., Schneider, M.D., Srivastava, D., and Olson, E.N. (2005). The Hand1 and Hand2 transcription factors regulate expansion of the embryonic cardiac ventricles in a gene dosage-dependent manner. Development *132*, 189-201.

McLean, C.Y., Bristor, D., Hiller, M., Clarke, S.L., Schaar, B.T., Lowe, C.B., Wenger, A.M., and Bejerano, G. (2010). GREAT improves functional interpretation of cis-regulatory regions. Nat Biotechnol *28*, 495-501.

Morikawa, Y., and Cserjesi, P. (2008). Cardiac neural crest expression of Hand2 regulates outflow and second heart field development. Circ Res *103*, 1422-1429.

Motenko, H., Neuhauser, S.B., O'Keefe, M., and Richardson, J.E. (2015). MouseMine: a new data warehouse for MGI. Mamm Genome *26*, 325-330.

Quinlan, A.R., and Hall, I.M. (2010). BEDTools: a flexible suite of utilities for comparing genomic features. Bioinformatics *26*, 841-842.

Robinson, M.D., McCarthy, D.J., and Smyth, G.K. (2010). edgeR: a Bioconductor package for differential expression analysis of digital gene expression data. Bioinformatics *26*, 139-140.

Srivastava, D., Thomas, T., Lin, Q., Kirby, M., Brown, D., and Olson, E. (1997). Regulation of cardiac mesodermal and neural crest development by the bHLH transcription factor, dHAND. Nat Genet *16*, 154-160.

Tsuchihashi, T., Maeda, J., Shin, C.H., Ivey, K.N., Black, B.L., Olson, E.N., Yamagishi, H., and Srivastava, D. (2011). Hand2 function in second heart field progenitors is essential for cardiogenesis. Dev Biol *351*, 62-69.

Visel, A., Minovitsky, S., Dubchak, I., and Pennacchio, L.A. (2007). VISTA Enhancer Browser--a database of tissue-specific human enhancers. Nucleic Acids Res *35*, D88-92.

VanDusen, N.J., Casanovas, J., Vincentz, J.W., Firulli, B.A., Osterwalder, M., Lopez-Rios, J., Zeller, R., Zhou, B., Grego-Bessa, J., De La Pompa, J.L.*, et al.* (2014). Hand2 is an essential regulator for two Notch-dependent functions within the embryonic endocardium. Cell Rep *9*, 2071-2083.

Zhang, Y., Liu, T., Meyer, C.A., Eeckhoute, J., Johnson, D.S., Bernstein, B.E., Nusbaum, C., Myers, R.M., Brown, M., Li, W.*, et al.* (2008). Model-based analysis of ChIP-Seq (MACS). Genome Biol *9*, R137.